applied sciences

MDPI

Review

Low-Light Photodetectors for Fluorescence Microscopy

Hiroaki Yokota [1,*], Atsuhito Fukasawa [2], Minako Hirano [1] and Toru Ide [3]

[1] Biophotonics Laboratory, The Graduate School for the Creation of New Photonics Industries, 1955-1 Kurematsu-cho, Nishi-ku, Hamamatsu-shi, Shizuoka 431-1202, Japan; hirano37@gpi.ac.jp
[2] Electron Tube Division, Hamamatsu Photonics K.K., 314-5 Shimokanzo, Iwata-shi, Shizuoka 438-0193, Japan; fukasawa@etd.hpk.co.jp
[3] Graduate School of Interdisciplinary Science and Engineering in Health Systems, Okayama University, 3-1-1 Tsushima-naka, Kita-ku, Okayama-shi, Okayama 700-8530, Japan; ide@okayama-u.ac.jp
* Correspondence: yokota@gpi.ac.jp

Abstract: Over the years, fluorescence microscopy has evolved and has become a necessary element of life science studies. Microscopy has elucidated biological processes in live cells and organisms, and also enabled tracking of biomolecules in real time. Development of highly sensitive photodetectors and light sources, in addition to the evolution of various illumination methods and fluorophores, has helped microscopy acquire single-molecule fluorescence sensitivity, enabling single-molecule fluorescence imaging and detection. Low-light photodetectors used in microscopy are classified into two categories: point photodetectors and wide-field photodetectors. Although point photodetectors, notably photomultiplier tubes (PMTs), have been commonly used in laser scanning microscopy (LSM) with a confocal illumination setup, wide-field photodetectors, such as electron-multiplying charge-coupled devices (EMCCDs) and scientific complementary metal-oxide-semiconductor (sCMOS) cameras have been used in fluorescence imaging. This review focuses on the former low-light point photodetectors and presents their fluorescence microscopy applications and recent progress. These photodetectors include conventional PMTs, single photon avalanche diodes (SPADs), hybrid photodetectors (HPDs), in addition to newly emerging photodetectors, such as silicon photomultipliers (SiPMs) (also known as multi-pixel photon counters (MPPCs)) and superconducting nanowire single photon detectors (SSPDs). In particular, this review shows distinctive features of HPD and application of HPD to wide-field single-molecule fluorescence detection.

Keywords: low-light photodetectors; fluorescence microscopy; time-resolved fluorescence microscopy; hybrid photodetector (HPD); single-molecule fluorescence detection

Citation: Yokota, H.; Fukasawa, A.; Hirano, M.; Ide, T. Low-Light Photodetectors for Fluorescence Microscopy. *Appl. Sci.* **2021**, *11*, 2773. https://doi.org/10.3390/app11062773

Academic Editor: Jacek Wojtas

Received: 19 February 2021
Accepted: 17 March 2021
Published: 19 March 2021

1. Introduction

The development of the light microscope has enabled investigation of the fine structures of biological specimens under magnification. In recent decades, fluorescence microscopy—a form of highly sensitive optical microscopy—has evolved and is a necessary element of life science studies [1–3]. Microscopy has elucidated biological processes in vitro and in vivo, and also enabled tracking of biomolecules in real time. Development of highly sensitive photodetectors and light sources, in addition to evolution of various illumination methods and fluorophores, has helped microscopy acquire single-molecule fluorescence sensitivity, enabling single-molecule fluorescence imaging and detection [4–7]. Single-molecule fluorescence microscopy led to the emergence of super-resolution microscopy [8–10].

Low-light photodetectors used in fluorescence microscopy are classified into two categories: point photodetectors and wide-field photodetectors [5,11]. Point photodetectors, notably photomultiplier tubes (PMTs), are most commonly used in laser scanning microscopy (LSM). The detectors are also used in point-like excitation and detection to study freely diffusing biomolecules, such as protein molecules and nucleic acids (DNA and

RNA) in solution [11]. Wide-field photodetectors, such as electron-multiplying charge-coupled devices (EMCCDs) and scientific complementary metal-oxide-semiconductor (sCMOS) cameras, are used in wide-field illumination and detection to study surface-immobilized or slowly-diffusing biomolecules and organelles. These biomolecules and organelles include protein molecules, nucleic acids, and lipids, and nucleus and mitochondria, respectively. The two photodetectors are distinct in many aspects. Point photodetectors have high temporal resolution (high sampling frequency) but have no spatial resolution without scanning. Wide-field photodetectors, in contrast, have spatial resolution (typically sub-micrometer precision) but are limited to relatively low frame rates. This review focuses on low-light point photodetectors and presents their fluorescence microscopy applications and recent progress.

In fluorescence microscopy, the fluorescence emission can be characterized not only by intensity and position but also by lifetime [12]. Fluorescence microscopy uses two fluorescence detection methods: steady-state and time-resolved fluorescence detection. Time-resolved measurements contain more information than is available from steady-state measurements. Fluorescence lifetime measurement by time-resolved detection provides data that is independent of fluorophore concentration and allows us to obtain information on the local ambient environment around the fluorophore, such as pH, ion concentrations, temperature, and fluorescence resonance energy transfer (FRET) efficiency [13]. The laser scanning fluorescence microscope, an indispensable imaging device in the biological sciences, is one of the most widely used fluorescence microscopy. LSM with a confocal illumination setup provides a base for various fluorescence microscopes using steady-state and time-resolved fluorescence detection, such as two-photon microscopy and fluorescence lifetime imaging microscopy (FLIM). This review introduces these point detectors, describes their operating principles, and compares their specifications. These photodetectors include conventional PMTs, single photon avalanche diodes (SPADs), hybrid photodetectors (HPDs), in addition to newly emerging multi-pixel photon counters (MPPCs) (also known as silicon photomultipliers (SiPMs)) and superconducting nanowire single photon detectors (SSPDs). In particular, this review shows distinctive features of HPD, and notes the applications of HPD to wide-field single-molecule fluorescence detection and the development of multi-pixel photodetectors.

2. Fluorescence Microscopy

Fluorescence measurements are characterized by their high sensitivity, up to single-molecule detection. Because biological samples commonly exhibit low contrast, fluorescence microscopy makes good use of fluorescence phenomenon to enhance the contrast. Fluorescence microscopy acquires data of target biological samples through fluorescence emissions characterized not only by intensity and position, but also by lifetime. Fluorescence microscopy uses the two fluorescence detection methods: steady-state and time-resolved fluorescence detection. LSM with a confocal illumination setup provides a base for various fluorescence microscopes using steady-state and time-resolved fluorescence detection, such as two-photon microscopy and FLIM.

2.1. Fluorescence

Fluorescence is a photophysical phenomenon of the emission of light through the excitation of a fluorophore from the ground state to an excited electronic state upon the absorption of light, with the light energy equivalent to the energy gap between the two states [10,12]. Figure 1 shows a Jablonski diagram that illustrates the electronic energy levels of a fluorophore and the transitions between them are represented by arrows. S_0, S_1, and S_2 represent the singlet ground, and first and second excited electronic states, respectively. The vibrational ground states and higher vibrational states of each electronic state are illustrated with black and gray lines, respectively. The transition from the ground state to the excited state by the light absorption occurs in less than 10^{-15} s. A fluorophore is usually excited to some higher vibrational level of the excited state. The electron usually

rapidly relaxes to the lowest vibrational level of S_1. This process is called internal conversion and generally occurs within 10^{-12} s. Then, the excited state is relaxed to the ground state in a few nanoseconds (10^{-9} s), which is accompanied by the radiation of the fluorescence emission. Because internal conversion is generally complete prior to emission, the last relaxation step to the ground state accounts for most of the overall process. Thus, the relaxation time is called the fluorescence lifetime. The wavelength of the fluorescence is longer than the excitation wavelength because the energy from the absorbed photon is partially lost via non-radiative decay. This shift in wavelength is called the Stokes shift.

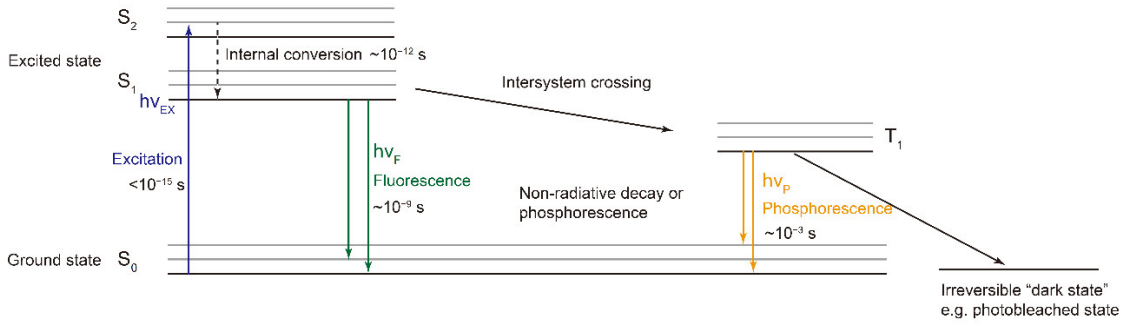

Figure 1. Jablonski diagram for the electronic energy levels of a fluorophore and the transitions between them.

An electron in the S_1 state can also flip its spin thus creating the first triplet state T_1, which is termed intersystem crossing. Transition from T_1 to S_0 is forbidden, thus the rate constants for triplet emission (phosphorescence) are several orders of magnitude smaller than those for fluorescence, which results in a long-lived dark state called blinking. While in the T_1 state, the fluorophore may experience photobleaching, which is an irreversible fluorescence switching-off process.

Table 1 shows characteristics of several fluorophores commonly used in fluorescence microscopy, including dyes, a quantum dot (Qdot) [14–16], and a fluorescent protein [17,18]. Photobleaching can be a representative photostability indicator of a fluorophore and the higher resistance to photobleaching allows longer or brighter fluorescence observation.

Table 1. Characteristics of fluorophores commonly used in fluorescence microscopy.

Fluorophore	Typical Excitation Wavelength (nm)	Emission Wavelength (nm)	Molecular Extinction Coefficient ($M^{-1}cm^{-1}$)	Quantum Yield	Fluorescence Lifetime (ns)	Resistance to Photoblea-Ching
Cy3	532	570	150,000 (550 nm)	0.15	0.2	++
Cy5	633	670	250,000 (649 nm)	0.28	0.9	++
Qdot655	532, 633	~655	2,100,000 (532 nm)	0.44	~20	+++
Green fluorescent protein (GFP)	488	507	56,000 (484 nm)	0.60	2.3	+

The markings +, ++, and +++ indicate "poor," "moderate," and "excellent," respectively. Adapted with permission from [7].

2.2. Laser Scanning Fluorescence Microscopy (LSM)

Laser scanning fluorescence microscopy (LSM) is one of the most widely used forms of biological fluorescence microscopy. LSM creates fluorescence images by sequentially recording the fluorescence intensity of each pixel by scanning a focused laser beam across a specimen using confocal optics to obtain only in-focus fluorescence. LSM with a confocal

illumination setup provides a base for various fluorescence microscopes using steady-state and time-resolved fluorescence microscopy. Figure 2 shows schematics of confocal microscopy and fluorescence microscopy with confocal optics.

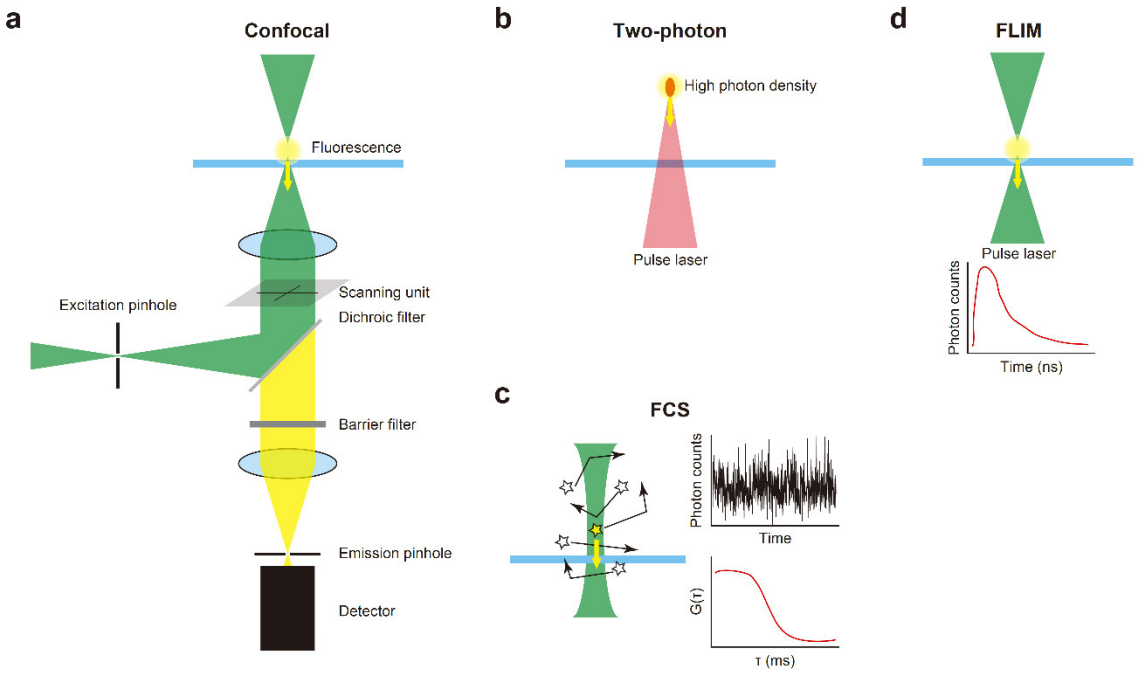

Figure 2. Schematics of confocal microscopy and fluorescence microscopy with confocal optics: (**a**) confocal microscopy; (**b**) two-photon microscopy; (**c**) fluorescence correlation microscopy (FCS); (**d**) fluorescence lifetime imaging microscopy (FLIM).

2.3. Confocal Microscopy

Confocal microscopy limits the observed volume to reduce out-of-focus signals. Minsky introduced the concept of confocal microscopy [19] and issued an original patent for a microscope in 1961. In confocal microscopy, two pinholes that are conjugated in the identical image plane are placed at a focal point in the light path. Light from outside of the focal plane is not focused on the pinhole(s) and only fluorescence very near to the sample's focal point reaches the detector (Figure 2a). Thus, the confocal laser scanning microscopy enables three dimensional reconstruction of specimens.

2.4. Two-Photon Micriscopy

Two-photon microscopy, which was first reported by the Watt W. Webb group in 1990 [20], makes use of the phenomenon that two photons are absorbed by a fluorophore simultaneously. The fluorophore can be excited by light with one-half the energy of each photon or twice the wavelength. The two-photon excitation light is generated by increasing the photon density using a focused high-power femtosecond pulse laser (Figure 2b). Fluorescence emitted from the focus point is detected by a point detector (commonly a PMT) and a fluorescence image is acquired by LSM. Two-photon microscopy enables deep imaging because the microscopy uses near-infrared laser excitation light that exhibits better tissue penetration and collects the localized fluorescence signal.

2.5. Fluorescence Correlation Spectroscopy (FCS)

Fluorescence correlation spectroscopy (FCS) is also based on confocal optics with a continuous wave laser(s) and monitors the mobility of molecules, typically translation diffusion into and out of a small volume (Figure 2c) [12]. FCS analyzes time-dependent fluorescence intensity fluctuations in a tiny observed volume on the order of femtoliter.

When a fluorophore diffuses (or fluorophores diffuse) into the illuminated volume, a fluorescence burst is detected due to steady-state fluorescence emission from the fluorophore(s). If the fluorophore diffuses (or fluorophores diffuse) quickly out of the volume, the burst duration is short, whereas if the fluorophore diffuses (or fluorophores diffuse) more slowly the photon burst duration persists for longer. Correlation analysis of the time series enables the diffusion coefficient of the fluorophore to be determined.

The fluorescence intensity fluctuation depends on the size and number of the molecules passing through the illuminated volume, which provides information on biomolecular interaction in vitro and in vivo.

2.6. Fluorescence Lifetime Imaging Microscopy (FLIM)

Fluorescence lifetime imaging microscopy (FLIM) is an advanced tool that maps the fluorescence lifetime distribution through time-resolved fluorescence detection (Figure 2d) [21,22]. The fluorescence lifetime can respond to changes in pH, temperature, and ion concentrations such as calcium concentration. Its capability to offer both localization of target fluorophores and the fluorophores' local microenvironment exhibits its superiority to fluorescence intensity based steady-state imaging because the lifetime of a fluorophore is mostly independent of its concentration. FLIM can be performed using the time-domain method in which the sample is excited with a pulse laser, or the frequency-domain method in which the sample is excited with intensity-modulated light, commonly sine-wave modulation [12].

3. Single Point Detectors

3.1. Performance Indices

3.1.1. Dark Count

Dark count refers to the tiny flow of electricity in a photodetector operated under a totally dark condition. This dark current should be minimized. Dark count is caused by several phenomena that vary with photodetectors. The dark count of PMTs results from thermionic emission from the photocathode and dynode, and ionization of residual gases (ion feedback) [23]. The dark count of SPADs and SiPMs results from thermionic emission from the depletion layer. The dark count of HPDs is negligible due to its high electron bombardment gain. The dark count of SSPDs, which is low and dependent on the cooling temperature and bias current [24], results from energy dissipation in the nanowire and the blackbody radiation at room temperature through the optical fiber [25].

3.1.2. Instrument Response Function

The transit time and its fluctuation are the major determinants of the time response of a photodetector [23]. The transit time refers to the travel time of the photoelectron. The full-width half-maximum (FWHM) of the instrument response function is a standard for the time response. Many detectors exhibit a non-Gaussian instrument response function. The rise and fall times of a detector are evaluated from the waveform. Transit time spread (TTS) is the fluctuation of the transit time of the single photoelectron pulse.

3.1.3. Afterpulse

Afterpulses are spurious pulses that may appear subsequent to the input signal [23]. An afterpulse is best characterized by the autocorrelation function of the detected photons. For vacuum tube-based photodetectors, positive ions generated by the ionization of residual gases in a detector create afterpulses that appear several hundreds of nanoseconds to several microseconds later than the input signal. This phenomenon is called ion feedback [23]. Among solid-state photodetectors, SPADs and SiPMs experience high afterpulse noise with high count rate measurements. The afterpulse noise is generated by thermally released trapped carriers [26]. HPDs and SSPDs are free of afterpulses.

3.1.4. Sensitivity

The sensitivity of a photodetector is largely determined by the quantum efficiency of the photocathode material. Most photocathodes used in vacuum tube-based photodetectors are made of compound semiconductors. GaAsP exhibits the highest quantum efficiency in the visible region (about 45%). A photocathode (extended red GaAsP) that is more sensitive to a longer wavelength than GaAsP is available for Hamamatsu Photonic products. Silicon and group III-V compound semiconductors, such as InGaAs and GaAs, are also used in solid-state photodetectors. Figure 3 shows the spectral response of these photocathodes.

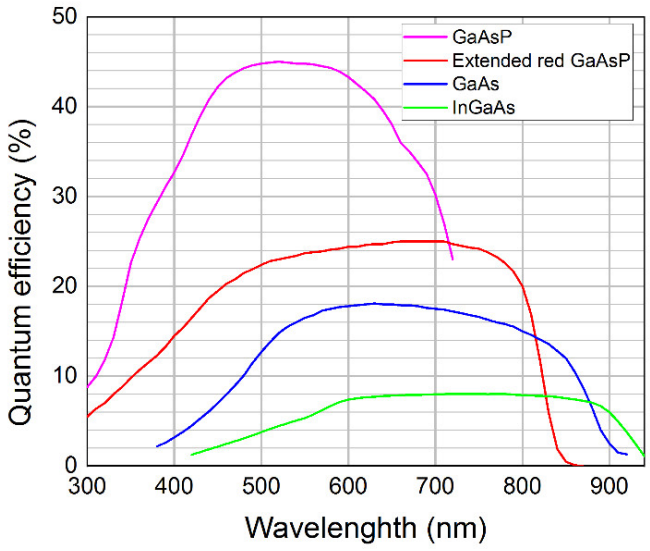

Figure 3. Spectral response of photocathodes.

These photocathodes are usually used in a vacuum and under the ambient temperature ranging from room temperature down to 273 K. As the ambient temperature is lowered, the spectra slightly shift to shorter wavelength due to the bandgap broadening of the semiconductors. Thus, the spectral response of these photocathodes does not change significantly in the temperature range.

3.1.5. Active Area

The diameter or surface of the active area of a photodetector determines the observed area. Confocal optics uses a pinhole in a plane conjugate with the image plane in the sample—the light from the pinhole is easy to focus on a small point detector, such as a SPAD [13]. Point photodetectors with a larger active area are often useful because the light does not need to be focused and they can used to observe a large area without scanning.

3.2. Photomultiplier Tube (PMT)

Photomultiplier tubes (PMTs) are the most widely used point detectors in fluorescence microscopy. A PMT is a vacuum tube that contains a photocathode, focusing electrodes, an electron multiplier (dynodes), and an anode (Figure 4) [23]. Incident photons are absorbed by the photocathode, which ejects primary electrons (~3 eV). The electrons are accelerated by a high voltage to hit a series of dynodes. Then, additional electrons (5–10 electrons) are ejected and exponentially amplified. The electron current is then detected by an external electrical circuit. Typical PMTs have 8–10 dynodes with a cathode-to-anode voltage gap of ~1 kV and current gain of 10^6 to 10^7.

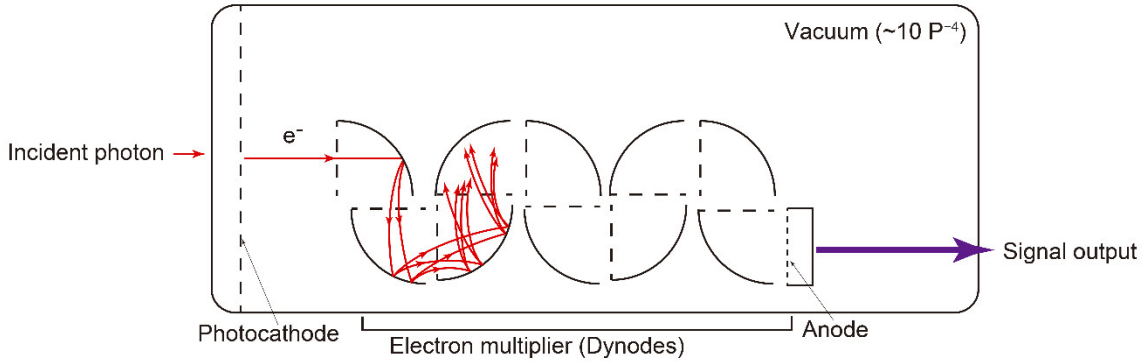

Figure 4. Schematic of a photomultiplier tube (PMT).

The main photocathodes used in PMTs are bi-alkali, with spectral response peaks around 400 nm and range of up to 700 nm. The advent of the GaAsP photocathode with its spectral response peak around 500 nm invigorated the LSM market because its spectral response ranges from visible light (500–700 nm) to near infrared light (900 nm). Laser scanning microscopes with a GaAsP photocathode were released to the market in the late 2000s. Current laser scanning microscopes incorporate PMTs with these multi-alkali photocathodes.

PMTs have been the leading low-light point photodetector for some time and, thus, a large number of power supplies and signal processing circuits for them are available. However, troubles can arise from unwanted noise generated by residual gas molecules (ion feedback), and large variation in responsivity and gain caused by difficulty in controlling metal evaporation to produce photocathodes and secondary electron surfaces. In addition, single photons can be detected with PMTs, but discrimination of single versus multiple photons is difficult.

3.3. Single Photon Avalanche Diode (SPAD)

The single photon avalanche diode (SPAD) is a solid-state photodetector composed of three semiconductor layers, called p-layer, i-layer, and n-layer (Figure 5) [27]. The n-layer has extra electrons, whereas the p-layer has holes. The average gain for an avalanche photodiode (APD) is around 100, which is insufficient for single-photon detection. Therefore, SPADs are usually operated in "Geiger-mode," where an applied bias voltage is greater than the diode's breakdown voltage. Then, when a charge is generated by an incident photon, the charge multiplication (or avalanche) occurs until it saturates corresponding to a current typically specified by the components. These APDs with a single pixel are referred to as SPADs, and those with multiple pixels are referred to as silicon photomultipliers (SiPMs) or multi-pixel photon counters (MPPCs). Although Geiger-mode driven SPADs are suitable for single photon counting, SPADs suffer several drawbacks. The active area cannot be increased because fabrication of a large semiconductor surface increases the number of defects. Geiger-mode driven SPADs have high dark counts due to the Geiger discharge and high afterpulse noise. The dead time is relatively long (about 50

ns), during which photon counting is inoperative because the mode needs to be reset for every single photon detection. To reduce dark counts, SPADs are typically cooled to 210–250 K.

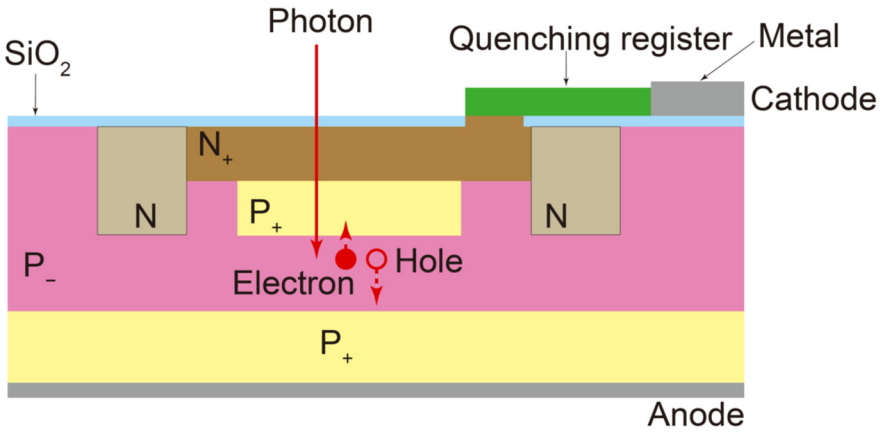

Figure 5. Schematic of a single photon avalanche diode (SPAD).

3.4. Hybrid Photodetector (HPD)

The hybrid photodetector (HPD) is a hybrid of an avalanche diode (AD) and a photocathode, both of which are in a vacuum tube (Figure 6) [23,26,28–31]. When light is incident onto the photocathode, photoelectrons are emitted from the photocathode. The photoelectrons are then accelerated by a high negative voltage to directly bombard the AD where electron-hole pairs are generated and the signal is amplified. The amplification is termed "electron bombardment gain".

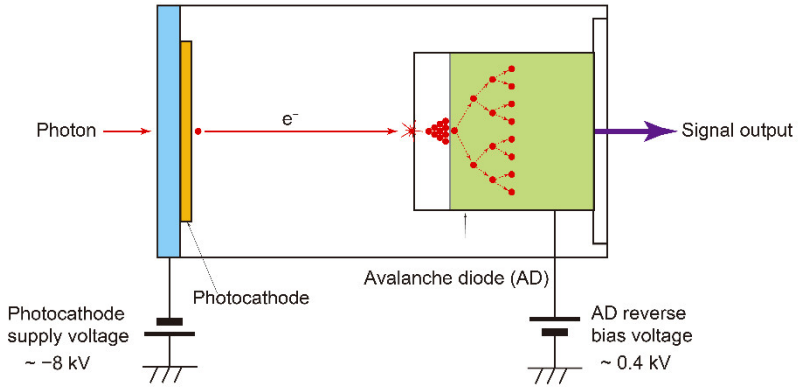

Figure 6. Schematic of a hybrid photodetector (HPD).

In the case of an HPD manufactured by Hamamatsu Photonics, the electron bombardment gain is approximately 1500 with the photocathode supply voltage of −8 kV. The signals of electron-hole pairs are further amplified to 80-fold (avalanche gain) by applying a reverse voltage of about 400 V to the avalanche diode. Then, the total gain will therefore be as much as about 120,000.

3.4.1. Features of HPD

HPDs have significant advantages over PMTs and other low-light photodetectors in the detection of fluorescence, as discussed below. However, a few disadvantages of HPDs also exist. The extremely high cathode supply voltage (−8 kV) is difficult to deal with, which can be problematic when incorporated into systems.

Low Afterpulse

HPDs have a notable feature of lower afterpulse due to their uncomplicated internal structure. Therefore, the major cause of afterpulses, i.e., ion feedback, is highly unlikely to occur in HPDs. Afterpulses evaluated for an HPD and a PMT are shown in Figure 7. This graph shows the probability at which afterpulses may be generated by a single photoelectron input. In contrast to the PMT's multiple afterpulses in a time range from 100 ns to 1 μs, this HPD exhibited only a small number of afterpulses in the time range.

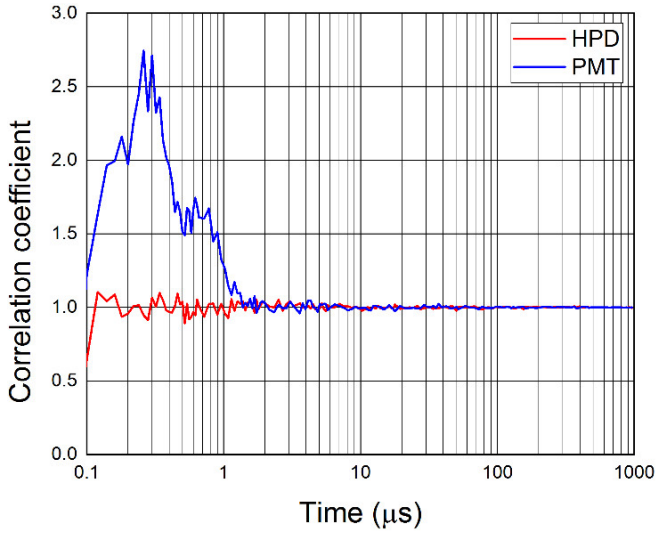

Figure 7. Afterpulse noise of PMT and HPD [32]. The data were obtained through detection of single photons from a continuous wave (CW) light source (wavelength = 470 nm). The cathode supply voltage and the reverse voltage of HPD were −8 kV and 398 V, respectively.

Comparable low afterpulses have been reportedly achieved solely for superconducting nanowire single photon detectors (SSPDs). These SSPDs have micrometer order active areas and must be operated at a liquid helium temperature [25], as discussed in Section 4.2.

High Resolution of Photon Counting

HPDs exhibit better pulse height resolution than PMTs. Gain fluctuation of HPDs is significantly lower owing to much higher electron bombardment gain (about 1500 at a photocathode supply voltage of −8 kV) than the first dynode gain of an ordinary photomultiplier tube (typically as low as 5–10). The first gain mostly determines the signal-to-noise ratio of the electron multiplication, which in turn represents the detector's capability to distinguish between one and multiple photons. As a result, HPDs offer high resolution of photon counting. As shown in Figure 8, signal peaks that correspond to 1, 2, 3, 4, and 5 photoelectrons can be identified in the output pulse height distribution.

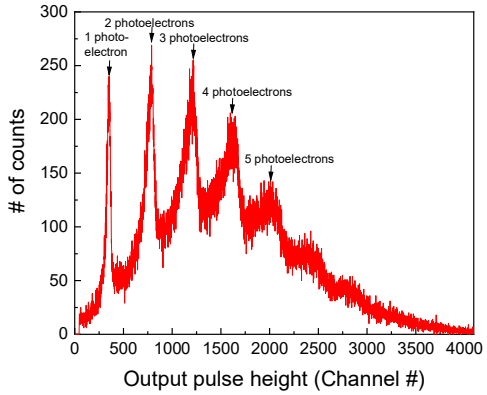

Figure 8. Output height distribution of an HPD [32]. The incident pulsed lights (wavelength = 470 nm) were adjusted to make the photocathode emit three photoelectrons on average. The cathode supply voltage and the reverse voltage were −8 kV and 380 V, respectively.

High Timing Resolution

Time response characteristics of HPDs are largely determined by the junction capacitance of the internal avalanche diode, provided the diameter of the internal avalanche diode is around or larger than 1 mm. The internal avalanche diode with a diameter of 1 mm and a very low capacitance (4 pF), which is incorporated in the current HPD product, realizes a fast response. Figure 9a shows the time response waveforms of an HPD and a PMT. The FWHM for the HPD is 0.6 ns, which is smaller than that for PMT (1.6 ns).

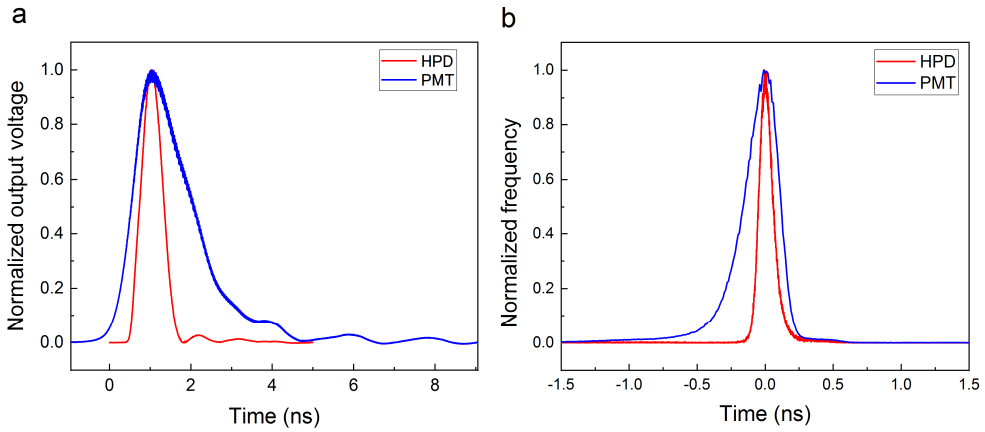

Figure 9. Time response characteristics of an HPD and a PMT [32]: (**a**) time response waveforms of an HPD and a PMT; (**b**) transit time spread (TTS) of an HPD and a PMT. The data were obtained using a pulse laser (wavelength = 405 nm) with a pulse width of 77 ps. The cathode supply voltage and the reverse voltage of HPD were −8 kV and 390 V, respectively.

The TTS determines the instrument response function of HPD. The following three factors mainly affect the TTS for HPD: (i) the transit time within the photocathode; (ii) the variation in the time taken for the photoelectrons to move in the vacuum from the photocathode to the avalanche diode; and (iii) the electron transit time within the avalanche diode. The TTS for an alkali photocathode is about 50 ps [31]. The measured raw TTS for a GaAsP photocathode in an HPD is about 113 ps, which is larger than that for alkali because the GaAsP layer is thicker than the alkali layer. This raw TTS value included the laser pulse width (77 ps) and temporal resolution of the measurement system (30 ps), so the net TTS should be much smaller. Figure 9b shows the time response waveforms of an HPD and a PMT. The raw TTS for the GaAsP photocathode in a PMT is 300 ps, which is larger than that of an HPD. These characteristics are very important for time-resolved fluorescence detection because it contributes to accurate fluorescence lifetime measurement.

Large Active Area

HPDs have a large effective area of more than several millimeters in diameter, enabling high photon collection efficiency. The active area of HPDs is comparable with that of PMTs, which is a marked contrast to SPADs with an effective diameter of only 10 micrometers.

Table 2 lists the characteristics of PMTs, SPADs, and HPDs.

Table 2. Characteristics of point photodetectors [23,27,32].

	Photomultiplier Tube (PMT)	Single Photon Avalanche Diode (SPAD)	Hybrid Photodetector (HPD)
Afterpulse	High	High	Low
Transit time spread (TTS)	~300 ps	~300 ps	~100 ps
Diameter of active area	~5 mm	~several 100 μm	~5 mm
Operating temperature	~270 K	210–250 K	Room temperature

3.4.2. HPD and Fluorescence Microscopy

The features of HPDs mentioned in Section 3.4.1 show the preeminence of HPDs in fluorescence microscopy applications, such as LSM, FLIM, and FCS. In practice, HPDs are incorporated into commercial microscopes and products of Becker & Hickl GmbH and PicoQuant.

FCS

In FCS, the presence of afterpulses deforms the correlation spectra. To avoid this issue, the fluorescence signal is commonly divided into two and detected by two detectors, and the cross-correlation between the two signals is calculated. This procedure is complicated and decreases the signal-to-noise ratio of each acquired datapoint. In contrast, the afterpulse-free feature of the HPD makes FCS measurement simpler, and a single HPD provides better data than PMT [13,26]. As shown in Figure 10, the autocorrelation spectrum acquired by an HPD is of good quality, whereas the spectrum acquired by PMT contains overlapped afterpulse noise below the 2 μs region.

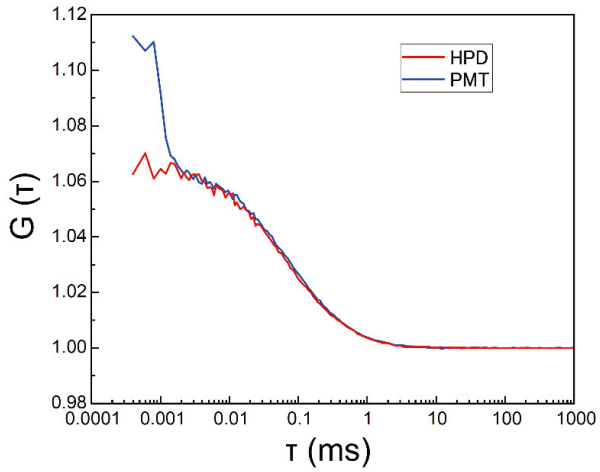

Figure 10. Autocorrelation data obtained by an HPD and a PMT [32]. The data were acquired using 100 nM Alexa Fluor 532 dye solution.

FLIM

FLIM utilizes time-correlated single photon counting (TCSPC) and acquires higher temporal resolution data (<ns) than FCS. Figure 11 shows a comparison of fluorescence lifetime measurement data obtained by an HPD and a PMT. Afterpulses are also problem-

atic for FLIM. The afterpulse raises the baseline of the PMT data. Consequently, the dynamic range of PMT is lower by an order of magnitude than that of HPD and seriously interrupts determination of the decay time constant.

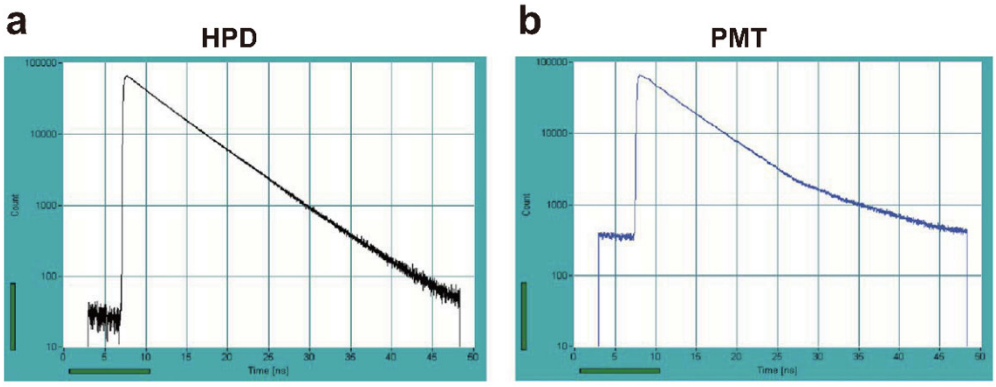

Figure 11. Fluorescence lifetime measurement data obtained by an HPD (**a**) and a PMT (**b**). The data were acquired using fluorescein dye solution. Adapted with permission from [13].

Compared with SPADs, HPDs can obtain brighter FLIM images due to the larger active area of the HPD. Figure 12 shows FLIM images acquired by an HPD and a SPAD. Although the quantum yields of the photodetectors were similar, the image acquired by the HPD collected twice as many photons as acquired by the PMT.

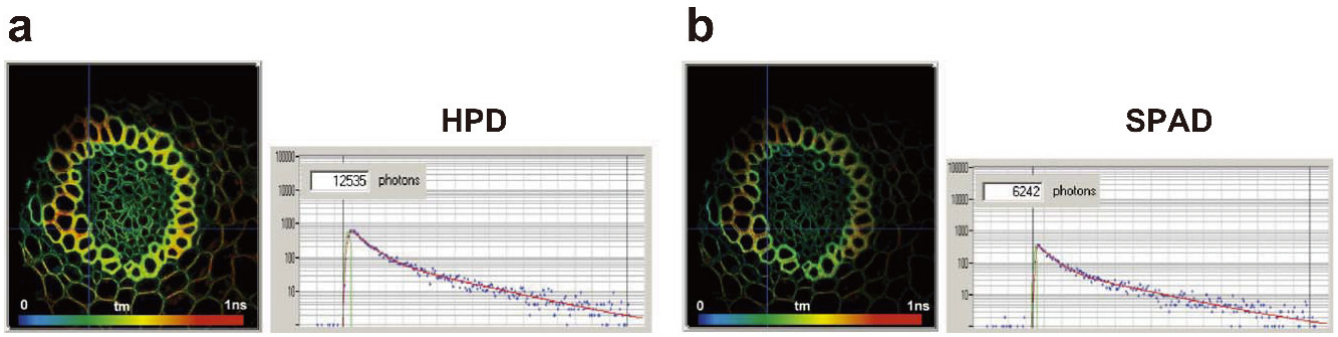

Figure 12. FLIM images acquired by HPD (**a**) and SPAD (**b**). Adapted with permission from [13].

3.4.3. Other Types of HPDs

This subsubsection briefly refers to other types of HPDs that were developed by Hamamatsu Photonics (Table 3) and applications of the HPD to single-molecule fluorescence microscopy. These other types of HPDs are cooled HPD and MPPC (SiPM)-incorporated HPDs.

Table 3 lists the characteristics of these HPDs.

Table 3. Other types of HPDs [32–35].

Type of HPD	Feature	Possible Application
Photocathode-cooled	Low thermal noise	FCS
MPPC (SiPM)-incorporated	Low voltage operation	Easy to install into systems

The cooled HPD, in which the photocathode is cooled by the Peltier element, reduces thermal electronic noise from the photocathode to one-tenth that of the non-cooled HPDs (Figure 13). This HPD is supposed to be useful for the detection of extremely low light, including single molecule detection.

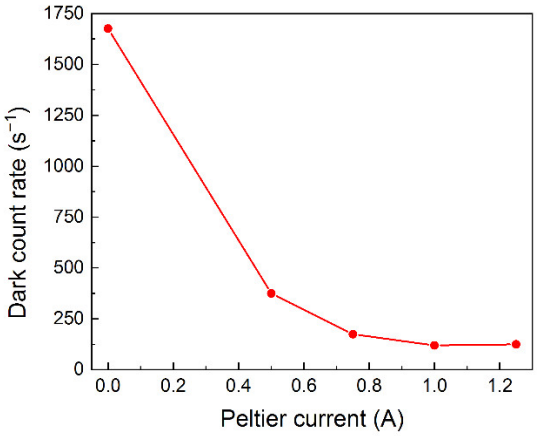

Figure 13. Dependence of dark count rate of the developed cooled HPD on the applied Peltier current [32]. Application of 1.2 A Peltier current cooled the HPD to about 283 K at an ambient temperature of 298 K.

The MPPC-incorporated HPD was developed to solve the difficulties of operating the HPD under high voltages such as 8 kV. The MPPC-incorporated HPD can operate with a lower voltage that operates PMTs due to the MPPC's high gain, and is able to detect single photons. The first prototype of an MPPC (SiPM)-incorporated HPD with a GaAsP photocathode with a diameter of 3 mm and a 25.4-mm (1-inch) bi-alkali photocathode type of MPPC (SiPM)-incorporated HPD were developed by Hamamatsu Photonics, and Barbato et al. evaluated its characteristics [33,34]. As shown in Figure 14, the HPD operates with lower voltages (photocathode voltage ~−3 kV and MPPC bias voltage ~ +70 V) than those of the current HPD product that incorporates an AD (photocathode voltage ~−8 kV and avalanche photodiode bias voltage ~+450 V). The low voltage operation capability facilitates installation of the HPD into various apparatus, including fluorescence microscopes. Recently, Hamamatsu Photonics developed an HPD with a 50.8-mm (2-inch) diameter [35].

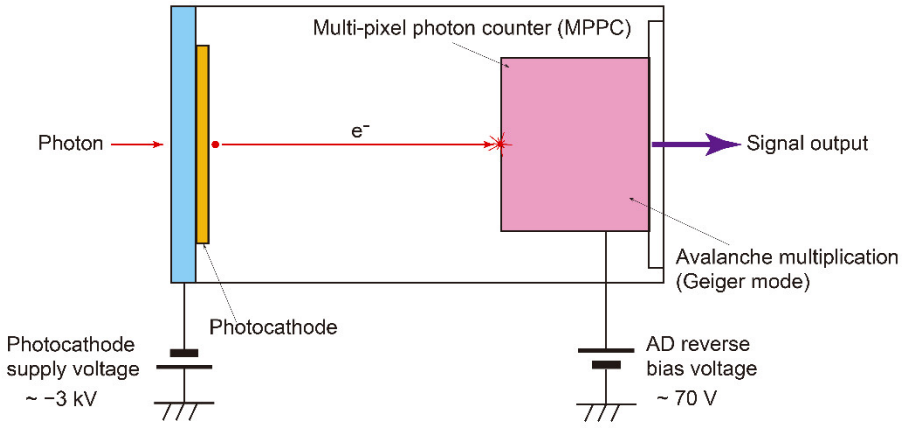

Figure 14. Schematic of multi-pixel photon counters (MPPC)-incorporated HPD.

3.4.4. Application of HPDs to Single-Molecule Fluorescence Microscopy

We applied the cooled-photocathode HPD to single-molecule fluorescence microscopy. We applied the HPD to low-background wide-field single-molecule fluorescence detection with high temporal resolution as a proof-of-principle demonstration. The fluorescence collected by an objective was divided into two, each simultaneously detected by HPD or imaged by EMCCD. The HPD allowed the fluorescence intensity of a mobile single molecule fluorophore to be determined at higher temporal resolution than conventional high-sensitivity CCD cameras. Specifically, the cooled-photocathode HPD detected fluorescence of a single Qdot while performing two-dimensional diffusion with 0.1 ms temporal resolution (Figure 15).

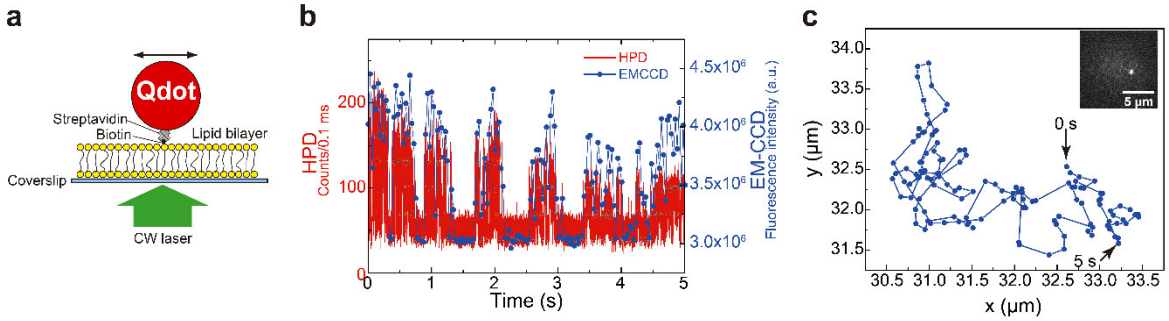

Figure 15. Wide-field sub-millisecond single-molecule fluorescence detection by a cooled HPD [32]: (**a**) Schematic of the observed mobile Qdot. The Qdot (Qdot655 streptavidin conjugate) was attached to biotinylated phosphoethanolamine (PE), 1,2-dioleoyl-sn-glycero-3-phosphoethanolamine-N-(cap biotinyl), via biotin-streptavidin interaction in a 1,2-dioleoyl-sn-glycero-3-phosphocholine (DOPC) lipid bilayer formed on a coverslip. The Qdot was excited by a CW laser (wavelength = 532 nm); (**b**) Time course of a mobile Qdot fluorescence intensity was obtained by an HPD with a time resolution of 0.1 ms (red). The repeated fluorescence-on and –off are caused by blinking. The intensity profile matches the intensity simultaneously obtained by EMCCD (blue) with a time resolution of 31.319 ms; (**c**) Trajectory of the Qdot obtained by EMCCD. The inset is a fluorescence image of the observed mobile Qdot.

The HPD also enabled wide-field single-molecule fluorescence lifetime measurement with nanosecond temporal resolution. We succeeded in obtaining time courses of fluorescence lifetime of a single Qdot whose fluorescence images were simultaneously monitored by an EMCCD (Figure 16).

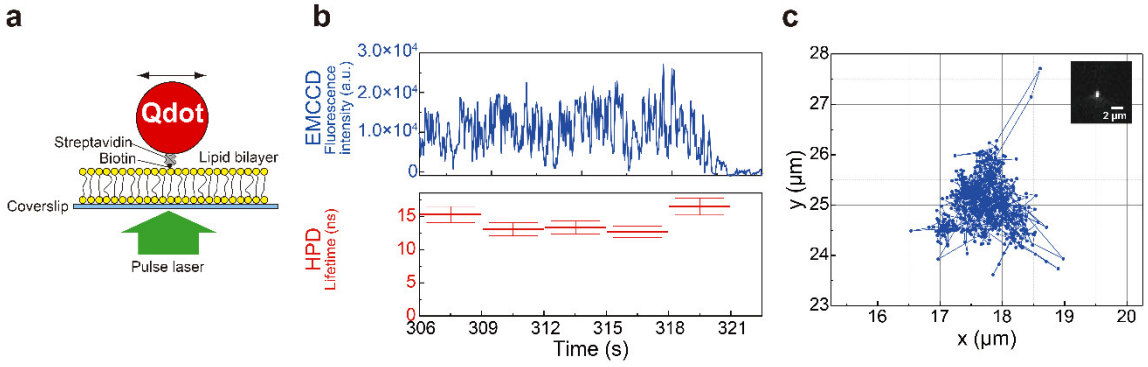

Figure 16. Wide-field single-molecule fluorescence lifetime measurement by a cooled HPD: (**a**) Schematic of the observed mobile Qdot. Sample preparation for the observation was identical to that described in the caption of Figure 15. The Qdot was excited by a pulse laser (wavelength = 520 nm); (**b**) Time courses of the Qdot fluorescence (upper, blue) obtained by an EMCCD and the lifetime (lower, red) simultaneously obtained by an HPD. The lifetime was obtained by fitting each decay curve drawn using data accumulated in three seconds with a single-exponential (red); (**c**) Trajectory of the Qdot obtained by EMCCD. The inset is a fluorescence image of the observed mobile Qdot.

A group at Tohoku University incorporated two HPDs into a specially equipped line confocal optical system in which a slit was used instead of a pinhole to improve the time

resolution of single-molecule FRET study. They achieved FRET observation of single protein molecules that flowed unidirectionally in a flow cell at a time resolution of 10 μs and analyzed the high-speed folding process of protein molecules [36].

4. Emerging Point Detectors

This section introduces newly emerging photodetectors that can be used for fluorescence microscopy. These photodetectors are silicon photomultipliers (SiPMs) also known as multi-pixel photon counters (MPPCs) and superconducting nanowire single photon detectors (SSPDs).

4.1. Silicon Photomultiplier (SiPM)

Silicon photomultipliers (SiPMs), which offer single photon detection capability, are an emerging photodetector in a variety of industries and biological fluorescence microscopy. Caccia summarized applications of SiPMs to biophotonics including fluorescence microscopy [37]. SiPM consist of a SPAD array. The sum of pulses from all SPADs is the SiPM output. Note that the number of SiPM output is single irrespective of the number of SPADs in the SiPM. Many photons can be simultaneously detected by the SPADs. Figure 17 shows a schematic of the operating principle of the SiPMs.

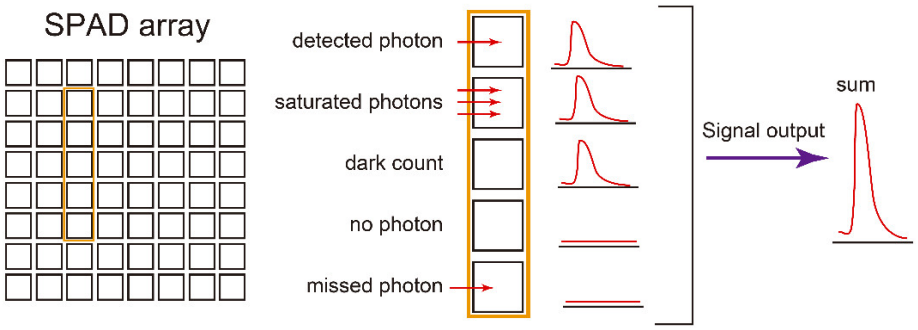

Figure 17. Schematic of the operating principle of silicon photomultipliers (SiPMs): SiPMs consist a SPAD array and every SPAD acts as an element that generates an all-or-nothing current pulse. When one or more photons are absorbed, a current pulse is generated. A current pulse is also produced by the dark count, whereas a current pulse is not generated when photon absorption fails. The output is the sum of the SPADs. Adapted with permission from [38] © The Optical Society.

SiPMs have several advantages over PMTs, including low fabrication cost, low operating voltage, and extremely high damage thresholds (high durability). In addition, silicon diodes have high quantum efficiency in the near-infrared region used for deep tissue imaging. Due to these factors, SiPMs can be better suited for high-speed imaging. Although SiPMs can detect intense light, their dark count rate is larger than that of PMTs, which is the major tradeoff. The advantage of high damage thresholds is reportedly distinct for confocal fluorescence microscopy and two-photon microscopy in clinical sites where surgical marking inks emit intense fluorescence [39]**.** SiPMs have not yet been widely used for biological imaging. Giacomelli et al. evaluated the performance of commercial SiPMs by comparing the SiPMs with a GaAsP PMT for LSM. They reported that the SiPM sensitivity exceeds the PMT sensitivity for moderate- to -highspeed LSM, whereas the PMT exhibited better sensitivity due to its lower dark counts for low speed LSM [39]. Modi et al. also compared SiPMs products with a GaAsP PMT for two-photon imaging of neural activity [38]. They showed that SiPM exhibited a signal-to-noise ratio that was comparable to or better than PMTs in usual calcium imaging, though dark counts of the SiPMs were higher than that of the PMT. They concluded that the low pulse height variability of the SiPMs surpassed the weak point and resulted in high performance.

4.2. SSPD

In recent decades, the superconducting nanowire single photon detector (SSPD) has become an increasingly popular device, with applications ranging from sensing to quantum communications for single photon detection with high efficiency, precise timing, and low noise [24,40]. The crucial high-speed feature of the SSPD is represented by the TTS (<50 ps) the fluctuation between the true arrival time of a photon and the electrically registered arrival time recorded by the system. Korzh et al. showed that the use of low-latency materials lowered the TTS of the SSPD, and demonstrated that the temporal resolution can be 2.6 ± 0.2 ps for visible wavelengths and 4.3 ± 0.2 ps at 1550 nm using a specialized niobium nitride SSPD [41].

Figure 18 shows a schematic of the SSPD. The SSPD consists of superconducting nanowire with a thickness of a few nanometers that senses photons. Single photon absorption by the SSPD suppresses superconductivity, which in turn generates a voltage spike that can be used to detect the photon.

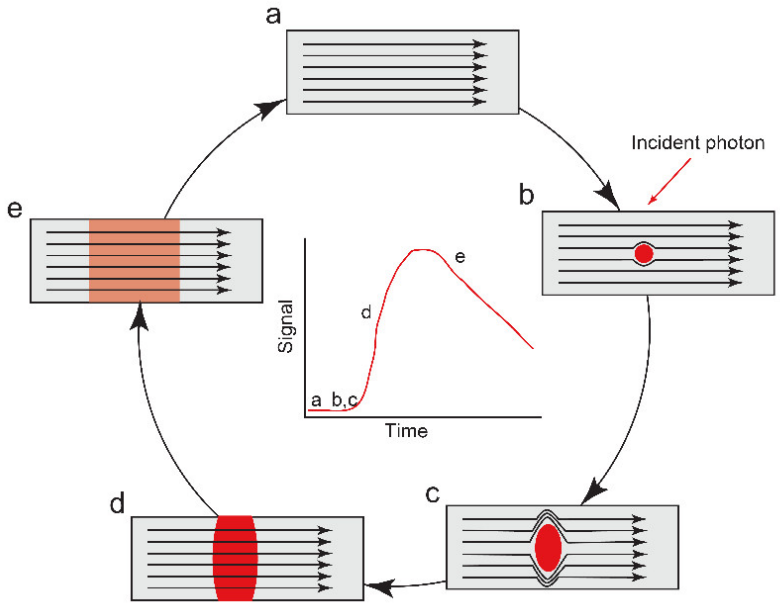

Figure 18. Schematic of the operating principle of the superconducting nanowire single photon detector (SSPD): The SSPD consists of a superconducting nanowire with a thickness of a few nanometers that senses photons. A bias electrical current flows through the nanowire during the operation: (**a**) the entire area is in the superconducting state prior to photon absorption; (**b**) single photon absorption takes place in the superconducting nanowire; (**c**) superconductivity is locally suppressed by energy excitation via the photon absorption; (**d**) the bias current makes the suppressed area resistive and the resistive area expands across the nanowire, which in turn generates a voltage spike; (**e**) as current is diverted, the resistive area relaxes to the superconducting state. Adapted with permission from [42]. Copyright 2020, American Chemical Society.

The SSPD is free of afterpulses because it returns to the superconducting state without generating afterpulses after photon detection. The afterpulsing-free characteristic of the SSPD is a clear advantage for time-resolved fluorescence microscopy. The SSPD has been used for fluorescence microscopy and applied to FCS [43,44]. Although the SSPD has these excellent features, its operation is inconvenient due to its small active area and low operating temperature. The very small active area (~10 μm) makes the optical alignment difficult and the extraordinary low operating temperature (≤4 K) requires the liquid helium cooling system.

Detailed comparisons have been made between SSPDs, SPADs, and other photon-counting technologies in [27,40,44].

The characteristics of SiPMs and SSPDs are summarized in Table 4.

Table 4. Characteristics of emerging photodetectors [24,27].

	SiPM	SSPD
Afterpulse	High	Low
Transit time spread (TTS)	~300 ps	~50 ps
Active area	~3 mm	~10 μm
Operating temperature	250 K–room temperature	≤4 K

5. Summary and Outlook

This paper provides an overview of low-light point photodetectors used in fluorescence microscopy and introduces several point detectors and their operating principles, focusing on HPDs that exhibit high timing resolution and low afterpulse. In addition, we demonstrate application of HPD to wide-field single-molecule fluorescence detection.

Fluorescence imaging with a point photodetector needs scanning to acquire an image and thus temporal resolution of the imaging is often limited. To overcome this limitation, excitation methods other than point excitation, such as multifocal excitation line excitation, have been proposed [45,46]. Regarding photodetectors, imagers with a large number of pixels have been reported by many groups [47–50]. For example, Zickus et al. reported scan-less wide-field FLIM using a camera consisting of a 500 × 1024 SPAD array at a rate of 1 Hz [51]. Michalet et al. firstly reported the evaluation of a multi-pixel (8 × 8) HPD developed by Hamamatsu Photonics [11]. Fukasawa, an author of this paper, and his colleagues, reported another multichannel HPD that was composed of 32 channels (two lines of 16 pixels) on a chip, in which the size of each pixel was 0.8 × 0.8 mm (Figure 19) [52]. It was confirmed that the timing resolution and afterpulse characteristics of the multichannel HPD are identical to the conventional single channel HPD. Wollman et al. reported an 1024-element SSPD array (a 32 × 32 row-column multiplexing architecture) [53]. Fast acquisition methods for FLIM and multi-pixel photodetectors have been reviewed by Liu et al. [22]. These point detector arrays can be widely applied to simultaneous multiparameter observation, including simultaneous multi-wavelength fluorescence observation.

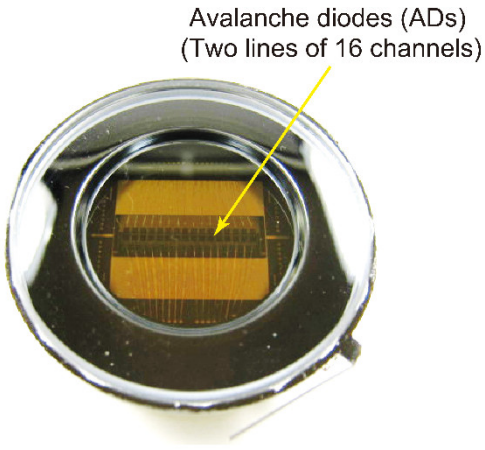

Figure 19. A photograph of the developed multichannel HPD. Adapted with permission from [52]. Copyright 2016, Elsevier.

Low-light photodetectors find more applications in various fields not limited to biological fluorescence microscopy [23]. These applications include flow cytometry and polymerase chain reaction (PCR) in life science, positron emission tomography (PET) for medical diagnosis, elementary particle (neutroino etc.) detection and collision experiments in high energy physics, and semiconductor wafer inspection in industry. In the near

future, combination of fluorescence microscopy and other modalities may make low-light photodetectors evolve further and may provide more detailed information on target biological specimens.

Author Contributions: Conceptualization, H.Y.; writing—original draft preparation, H.Y.; writing—review and editing, H.Y., A.F., M.H., and T.I.; investigation, H.Y. and A.F.; formal analysis, H.Y. and A.F.; supervision, H.Y.; visualization, H.Y. and A.F. All authors have read and agreed to the published version of the manuscript.

Funding: This work was supported by the Science Research Promotion Fund of the Promotion and Mutual Aid Corporation for Private Schools of Japan (to H.Y., M.H., and T.I.) and the research grant of Tokai Foundation for Technology (to H.Y. and A.F.).

Data Availability Statement: The data that support the findings of this study are available from the corresponding author upon reasonable request.

Acknowledgments: We would like to thank Yoshihiro Takiguchi for his advice on pulse lasers.

Conflicts of Interest: The author declares that there are no conflicts of interest. The funders had no role in the design of the study; in the collection, analyses, or interpretation of data; in the writing of the manuscript, or in the decision to publish the results.

Abbreviations

AD	avalanche diode
APD	avalanche photodiode
CW	continuous wave
DOPC	1,2-dioleoyl-sn-glycero-3-phosphocholine
EMCCD	electron-multiplying charge-coupled device
FCS	fluorescence correlation spectroscopy
FLIM	fluorescence lifetime imaging microscopy
FRET	fluorescence resonance energy transfer
FWHM	full-width half-maximum
GFP	green fluorescent protein
HPD	hybrid photodetector
LSM	laser scanning microscopy
MPPC	multi-pixel photon counter
PCR	polymerase chain reaction
PE	phosphoethanolamine
PET	positron emission tomography
PMT	photomultiplier tube
Qdot	quantum dot
sCMOS	scientific complementary metal-oxide-semiconductor
SiPM	silicon photomultiplier
SPAD	single photon avalanche diode
SSPD	superconducting nanowire single photon detector
TCSPC	time-correlated single photon counting
TTS	transit time spread

References

1. Lichtman, J.W.; Conchello, J.A. Fluorescence microscopy. *Nat. Methods* **2005**, *2*, 910–919.
2. Petty, H.R. Fluorescence microscopy: Established and emerging methods, experimental strategies, and applications in immunology. *Microsc. Res. Tech.* **2007**, *70*, 687–709.
3. Sanderson, M.J.; Smith, I.; Parker, I.; Bootman, M.D. Fluorescence microscopy. *Cold Spring Harb. Protoc.* **2014,** *2014*, pdb top071795.
4. Moerner, W.E.; Fromm, D.P. Methods of single-molecule fluorescence spectroscopy and microscopy. *Rev. Sci. Instrum.* **2003**, *74*, 3597–3619.

5. Michalet, X.; Siegmund, O.H.; Vallerga, J.V.; Jelinsky, P.; Millaud, J.E.; Weiss, S. Detectors for single-molecule fluorescence imaging and spectroscopy. *J. Mod. Opt.* **2007**, *54*, 239.
6. Shashkova, S.; Leake, M.C. Single-molecule fluorescence microscopy review: Shedding new light on old problems. *Biosci. Rep.* **2017**, *37*, BSR20170031.
7. Yokota, H. Fluorescence microscopy for visualizing single-molecule protein dynamics. *Biochim. Biophys. Acta Gen. Subj.* **2020**, *1864*, 129362.
8. Betzig, E.; Patterson, G.H.; Sougrat, R.; Lindwasser, O.W.; Olenych, S.; Bonifacino, J.S.; Davidson, M.W.; Lippincott-Schwartz, J.; Hess, H.F. Imaging intracellular fluorescent proteins at nanometer resolution. *Science* **2006**, *313*, 1642–1645.
9. Huang, B.; Wang, W.; Bates, M.; Zhuang, X. Three-dimensional super-resolution imaging by stochastic optical reconstruction microscopy. *Science* **2008**, *319*, 810–813.
10. Bertocchi, C.; Goh, W.I.; Zhang, Z.; Kanchanawong, P. Nanoscale Imaging by Superresolution Fluorescence Microscopy and Its Emerging Applications in Biomedical Research. *Crit. Rev. Biomed. Eng.* **2013**, *41*, 281–308.
11. Michalet, X.; Colyer, R.A.; Scalia, G.; Ingargiola, A.; Lin, R.; Millaud, J.E.; Weiss, S.; Siegmund, O.H.W.; Tremsin, A.S.; Vallerga, J.V.; et al. Development of new photon-counting detectors for single-molecule fluorescence microscopy. *Philos. Trans. R. Soc. B Biol. Sci.* **2013**, *368*, 20120035.
12. Lakowicz, J.R. *Principles of Fluorescence Spectroscopy*, 3rd ed.; Springer: Berlin/Heidelberg, Germany, 2006.
13. Becker, W.; Su, B.; Holub, O.; Weisshart, K. FLIM and FCS detection in laser-scanning microscopes: Increased efficiency by GaAsP hybrid detectors. *Microsc. Res. Tech.* **2011**, *74*, 804–811.
14. Michalet, X.; Pinaud, F.F.; Bentolila, L.A.; Tsay, J.M.; Doose, S.; Li, J.J.; Sundaresan, G.; Wu, A.M.; Gambhir, S.S.; Weiss, S. Quantum dots for live cells, in vivo imaging, and diagnostics. *Science* **2005**, *307*, 538–544.
15. Resch-Genger, U.; Grabolle, M.; Cavaliere-Jaricot, S.; Nitschke, R.; Nann, T. Quantum dots versus organic dyes as fluorescent labels. *Nat. Methods* **2008**, *5*, 763–775.
16. Kairdolf, B.A.; Smith, A.M.; Stokes, T.H.; Wang, M.D.; Young, A.N.; Nie, S. Semiconductor quantum dots for bioimaging and biodiagnostic applications. *Annu. Rev. Anal. Chem.* **2013**, *6*, 143–162.
17. Shaner, N.C.; Steinbach, P.A.; Tsien, R.Y. A guide to choosing fluorescent proteins. *Nat. Methods* **2005**, *2*, 905–909.
18. Shcherbakova, D.M.; Sengupta, P.; Lippincott-Schwartz, J.; Verkhusha, V.V. Photocontrollable fluorescent proteins for superresolution imaging. *Annu. Rev. Biophys.* **2014**, *43*, 303–329.
19. Minsky, M. Memoir on inventing the confocal scanning microscope. *Scanning* **1988**, *10*, 128–138.
20. Denk, W.; Strickler, J.H.; Webb, W.W. Two-photon laser scanning fluorescence microscopy. *Science* **1990**, *248*, 73–76.
21. Becker, W. Fluorescence lifetime imaging--techniques and applications. *J. Microsc.* **2012**, *247*, 119–136.
22. Liu, X.; Lin, D.; Becker, W.; Niu, J.; Yu, B.; Liu, L.; Qu, J. Fast fluorescence lifetime imaging techniques: A review on challenge and development. *J. Innov. Opt. Heal. Sci.* **2019**, *12*, 1930003.
23. Hamamatsu Photonics, K.K. *Editorial Committee, Photomultiplier Tubes Basic and Applications*, 4th ed.; Hamamatsu Photonics, K.K. Eds.; Electron Tube Division: Iwata-shi, Shizuoka, Japan, 2017.
24. Natarajan, C.M.; Tanner, M.G.; Hadfield, R.H. Superconducting nanowire single-photon detectors: Physics and applications. *Supercond. Sci. Technol.* **2012**, *25*, 063001.
25. Yamashita, T.; Miki, S.; Terai, H. Recent Progress and Application of Superconducting Nanowire Single-Photon Detectors. *IEICE Trans. Electron.* **2017,** *100*, 274–282.
26. Michalet, X.; Cheng, A.; Antelman, J.; Suyama, M.; Arisaka, K.; Weiss, S. Hybrid photodetector for single-molecule spectroscopy and microscopy. *Proc. Soc. Photo. Opt. Instrum. Eng.* **2008,** *6862*, doi:10.1117/12.763449.
27. Eisaman, M.D.; Fan, J.; Migdall, A.; Polyakov, S.V. Invited Review Article: Single-photon sources and detectors. *Rev. Sci. Instrum.* **2011**, *82*, 071101.
28. Suyama, M.; Kawai, Y.; Kimura, S.; Asakura, N.; Hirano, K.; Hasegawa, Y.; Saito, T.; Morita, T.; Muramatsu, M.; Yamamoto, K. A compact hybrid photodetector (HPD). *IEEE Trans. Nucl. Sci.* **1997**, *44*, 985.
29. Suyama, M.; Hirano, K.; Kawai, Y.; Nagai, T.; Kibune, A.; Saito, T.; Negi, Y.; Asakura, N.; Muramatsu, S.; Morita, T. A hybrid photodetector (HPD) with a III-V photocathode. *IEEE Trans. Nucl. Sci.* **1998**, *45*, 572.
30. Fukasawa, A.; Haba, J.; Kageyama, A.; Nakazawa, H.; Suyama, M. High Speed HPD for Photon Counting. In Proceedings of the 2006 IEEE Nuclear Science Symposium and Medical Imaging Conference, San Diego, CA, USA, 29 October–1 November 2006; Volume 1, pp. 43–47.
31. Fukasawa, A.; Haba, J.; Kageyama, A.; Nakazawa, H.; Suyama, M. High Speed HPD for Photon Counting. *IEEE Trans. Nucl. Sci.* **2008**, *55*, 758–762.
32. Fukasawa, A. Development and Promotion of Hybrid Photodetectors (HPDs) Used in Biological Fluorescence Microscopes. Doctoral Thesis, The Graduate School for the Creation of New Photonics Industries, Hamamatsu-shi, Shizuoka, Japan, 2016.
33. Barbarino, G.; Barbato, F.C.T.; Campajola, L.; Canfora, F.; de Asmundis, R.; De Rosa, G.; Di Capua, F.; Fiorillo, G.; Migliozzi, P.; Mollo, C.M.; et al. A new generation photodetector for astroparticle physics: The VSiPMT. *Astropar. Phys.* **2015**, *67*, 18–25.
34. Barbato, F.C.T.; Barbarino, G.; Campajola, L.; Di Capua, F.; Mollo, C.M.; Valentini, A.; Vivolo, D. R&D of a pioneering system for a high resolution photodetector: The VSiPMT. *Nucl. Instrum. Methods Phys. Res. A* **2017**, *876*, 48–49.
35. Fukasawa, A.; Hotta, Y.; Ishizu, T.; Negi, Y.; Nakano, G.; Ichikawa, S.; Nagasawa, T.; Egawa, Y.; Kageyama, A.; Adachi, I.; et al. Development of a new 2-inch hybrid photo-detector using MPPC. *Nucl. Instrum. Methods Phys. Res. A* **2018**, *912*, 290–293.

36. Oikawa, H.; Takahashi, T.; Kamonprasertsuk, S.; Takahashi, S. Microsecond resolved single-molecule FRET time series measurements based on the line confocal optical system combined with hybrid photodetectors. *Phys. Chem. Chem. Phys.* **2018**, *20*, 3277–3285.
37. Caccia, M.; Nardo, L.; Santoro, R.; Schaffhauser, D. Silicon Photomultipliers and SPAD imagers in biophotonics: Advances and perspectives. *Nucl. Instr. Meth. A* **2019**, *926*, 101–117.
38. Modi, M.N.; Daie, K.; Turner, G.C.; Podgorski, K. Two-photon imaging with silicon photomultipliers. *Opt. Express* **2019**, *27*, 35830–35841.
39. Giacomelli, M. Evaluation of silicon photomultipliers for multiphoton and laser scanning microscopy. *J. Biomed. Opt.* **2019**, *24*, 106503.
40. Hadfield, R.H. Single-photon detectors for optical quantum information applications. *Nat. Photon.* **2009**, *3*, 696–705.
41. Korzh, B.; Zhao, Q.-Y.; Allmaras, J.P.; Frasca, S.; Autry, T.M.; Bersin, E.A.; Beyer, A.D.; Briggs, R.M.; Bumble, B.; Colangelo, M.; et al. Demonstration of sub-3 ps temporal resolution with a superconducting nanowire single-photon detector. *Nat. Photon.* **2020**, *14*, 250–255.
42. Allmaras, J.P.; Wollman, E.E.; Beyer, A.D.; Briggs, R.M.; Korzh, B.A.; Bumble, B.; Shaw, M.D. Demonstration of a Thermally Coupled Row-Column SNSPD Imaging Array. *Nano Lett.* **2020**, *20*, 2163–2168.
43. Yamashita, T.; Liu, D.; Miki, S.; Yamamoto, J.; Haraguchi, T.; Kinjo, M.; Hiraoka, Y.; Wang, Z.; Terai, H. Fluorescence correlation spectroscopy with visible-wavelength superconducting nanowire single-photon detector. *Opt. Express* **2014**, *22*, 28783–28789.
44. Yamamoto, J.; Oura, M.; Yamashita, T.; Miki, S.; Jin, T.; Haraguchi, T.; Hiraoka, Y.; Terai, H.; Kinjo, M. Rotational diffusion measurements using polarization-dependent fluorescence correlation spectroscopy based on superconducting nanowire single-photon detector. *Opt. Express* **2015**, *23*, 32633–32642.
45. Yang, W.; Miller, J.E.; Carrillo-Reid, L.; Pnevmatikakis, E.; Paninski, L.; Yuste, R.; Peterka, D.S. Simultaneous Multi-plane Imaging of Neural Circuits. *Neuron* **2016**, *89*, 269–284.
46. Kazemipour, A.; Novak, O.; Flickinger, D.; Marvin, J.S.; Abdelfattah, A.S.; King, J.; Borden, P.M.; Kim, J.J.; Al-Abdullatif, S.H.; Deal, P.E.; et al. Kilohertz frame-rate two-photon tomography. *Nat. Methods* **2019**, *16*, 778–786.
47. Colyer, R.; Scalia, G.; Villa, F.; Guerrieri, F.; Tisa, S.; Zappa, F.; Cova, S.; Weiss, S.; Michalet, X. Ultra High-Throughput Single Molecule Spectroscopy with a 1024 Pixel SPAD. *Proc. SPIE Int. Soc. Opt. Eng.* **2011**, *7905*, 790503.
48. Michalet, X.; Ingargiola, A.; Colyer, R.A.; Scalia, G.; Weiss, S.; Maccagnani, P.; Gulinatti, A.; Rech, I.; Ghioni, M. Silicon photon-counting avalanche diodes for single-molecule fluorescence spectroscopy. *IEEE J. Sel. Top Quantum Electron.* **2014**, *20*, 38044201–380442020.
49. Antolovic, I.M.; Burri, S.; Bruschini, C.; Hoebe, R.A.; Charbon, E. SPAD imagers for super resolution localization microscopy enable analysis of fast fluorophore blinking. *Sci. Rep* **2017**, *7*, 44108.
50. Yabuno, M.; Miyajima, S.; Miki, S.; Terai, H. Scalable implementation of a superconducting nanowire single-photon detector array with a superconducting digital signal processor. *Opt. Express* **2020**, *28*, 12047–12057.
51. Zickus, V.; Wu, M.L.; Morimoto, K.; Kapitany, V.; Fatima, A.; Turpin, A.; Insall, R.; Whitelaw, J.; Machesky, L.; Bruschini, C.; et al. Fluorescence lifetime imaging with a megapixel SPAD camera and neural network lifetime estimation. *Sci. Rep* **2020**, *10*, 20986.
52. Fukasawa, A.; Egawa, Y.; Ishizu, T.; Kageyama, A.; Kamiya, A.; Muramatsu, T.; Nakano, G.; Negi, Y. Multichannel HPD for high-speed single photon counting. *Nucl. Instrum. Methods Phys. Res. A* **2016**, *812*, 81–85.
53. Wollman, E.E.; Verma, V.B.; Lita, A.E.; Farr, W.H.; Shaw, M.D.; Mirin, R.P.; Woo Nam, S. Kilopixel array of superconducting nanowire single-photon detectors. *Opt. Express* **2019**, *27*, 35279–35289.